

Dynamic Analysis of Girder Bridges

EUI-SEUNG HWANG AND ANDRZEJ S. NOWAK

This paper deals with the calculation of dynamic loads in girder bridges. Three major elements are considered: vehicle dynamics, road roughness, and bridge dynamics. The parameters representing the road profile and axle weights are treated as random variables. The statistical models are established on the basis of the available test, measurement, and analytical data. The mathematical equations relating forces and deformations are formulated, with the system of equations solved by a numerical integration method. Using the Monte Carlo technique, a procedure is developed for simulation of the dynamic load spectra. The approach is demonstrated on a typical steel girder bridge. The resulting distribution functions of the dynamic load are presented on a normal probability scale.

The dynamic load is an important parameter in bridge design and evaluation. In the current AASHTO standards (1), dynamic load (impact), I , is treated as an equivalent additional static load:

$$I = \left(\frac{50}{L + 125} \right) LL \tag{1}$$

where

- L = span length in ft and
- LL = live load.

In Ontario, the dynamic load allowance (fraction of live load) is specified as a function of the natural frequency of vibration of the bridge (2), as shown in Figure 1. A similar approach is used in the revised Swiss code (SIA 160) (3).

On the other hand, observations and measurements indicate that the dynamic behavior of the bridge is a function of three major factors (4-9):

- Dynamic properties of the vehicle (mass, suspension, axle configuration, tires, speed);
- Road roughness (approach, roadway, cracks, potholes, waves); and
- Dynamic properties of the bridge structure (span, mass, support types, material, geometry).

In this study a procedure is developed to quantify the dynamic load effect. The three factors just listed are considered. The analysis is performed for the superstructure of a simply supported girder bridge. The dynamic load effect in a bridge is measured in terms of a dynamic load factor (DLF). DLF is defined as the ratio of the maximum deflection experienced by the bridge (including dynamic effects) and the maximum

static deflection at midspan. Mathematical equations relating forces and deformations are formulated and solved using a numerical integration method. A simulation procedure, based on Monte Carlo technique, is developed to calculate the bridge dynamic load spectra.

The proposed procedure can be used for the development of more efficient design and evaluation criteria.

VEHICLE DYNAMICS

From the dynamic analysis point of view, the truck is composed of the body, wheels with tires, and the suspension system. There is a variety of configurations, including tractor with or without trailer(s) and different axle loads and axle spacings. In this study the four most common vehicles are used: two single trucks (S2 and S3) and two semi tractor-trailers (T4 and T5) as shown in Figure 2.

It is assumed that trucks are equipped with multileaf spring type suspensions. Leaf springs can be treated as nonlinear devices that dissipate energy during each cycle of oscillation. Their characteristics were measured by Fancher et al. (10). The results show that the force-deflection relationship does not depend on the frequency of oscillations occurring in the 0 to 15 Hz range, but it depends on the motion amplitude and the nominal load. Fancher et al. (10) derived nonlinear (logarithmic) equations relating forces and deflections of the truck suspension system. These equations are used in simulation of the DLF.

Tires can be treated as linear elastic spring components. The spring constants were measured by Fancher and Ervin (11). A typical value of 10,000 lb per in. per tire is used in this study.

A truck body is represented by a distributed mass subjected to rigid body motions. Vertical displacements and pitching rotations are considered. A trapezoid mass distribution is assumed with a constant mass density ρ (Figure 3). The mass moment of inertia about the mass central axis is

$$I = \frac{ph^3 p^2 + 4pq + q^2}{36 p + q} \tag{2}$$

where p , q , and h are shown in Figure 3. Let $r = c/(a + b)$ and W = total mass; then

$$I = W/6 [4(r^2 + r + 1)ab + (2r^2 + 2r - 1)(a^2 + b^2)] \tag{3}$$

where a , b , and c are dimensions also shown in Figure 3. A model of a single truck and the corresponding free body diagram are shown in Figure 4. Four equations can be obtained,

Department of Civil Engineering, The University of Michigan, Ann Arbor, Mich. 48109.

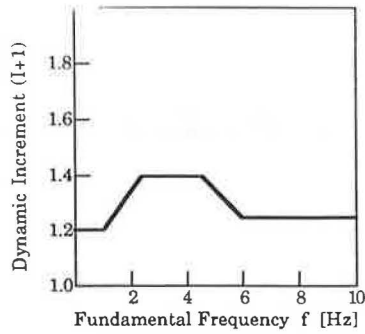


FIGURE 1 Dynamic load allowance in Ontario (2).

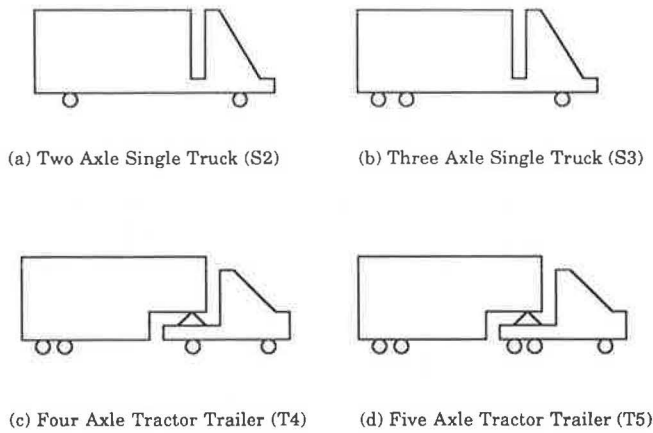


FIGURE 2 Trucks used in the study.

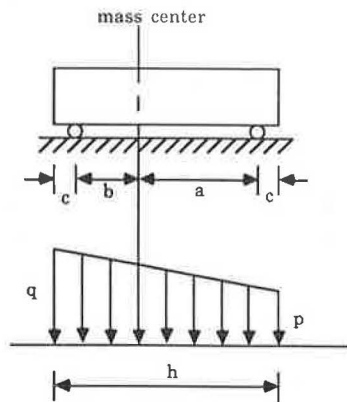


FIGURE 3 Truck body model.

three for the vertical equilibrium and one for the rotation equilibrium, as follows:

$$\begin{aligned}
 m_1(a_2\ddot{y}_1 + a_1\ddot{y}_2) + SF_1 + SF_2 &= 0 \\
 m_2\ddot{y}_3 + TF_1 - SF_1 &= 0 \\
 m_3\ddot{y}_4 + TF_2 - SF_2 &= 0 \\
 I_y(\ddot{y}_1 - \ddot{y}_2)/s + SF_1a_1s - SF_2a_2s &= 0
 \end{aligned}
 \tag{4}$$

where

- y_i = vertical displacements,
- m_i = masses,
- SF_i = suspension forces,
- TF_i = tire forces,
- s = distance between axles,
- a_i = distances between mass center and axles, and
- I_y = pitching rotation moment of inertia.

A model of a tractor-trailer and the corresponding free body diagram is shown in Figure 5. Seven equations can be obtained from the vertical and rotation equilibrium,

$$\begin{aligned}
 m_1\ddot{y}_{c1} + SF_1 + SF_2 + P_j &= 0 \\
 m_2\ddot{y}_{c2} + SF_3 - P_j &= 0 \\
 m_3\ddot{y}_4 + TF_1 - SF_1 &= 0 \\
 m_4\ddot{y}_5 + TF_2 - SF_2 &= 0 \\
 m_5\ddot{y}_6 + TF_3 - SF_3 &= 0 \\
 I_1\ddot{\theta}_1 + a_1s_1SF_1 - a_2s_1SF_2 - (a_3 - a_1)s_1P_j &= 0 \\
 I_2\ddot{\theta}_2 - a_6s_2SF_3 - a_5s_2P_j &= 0
 \end{aligned}
 \tag{5}$$

where

- s_i = distances between axles,
- P_j = tractor-trailer interaction force,
- y_{ci} = deflections at mass center,
- θ_i = rotations at mass center,
- I_i = pitching rotation moments of inertia, and other notations as in Equation 4.

From the truck geometry,

$$\begin{aligned}
 y_{c1} &= a_1y_2 + a_2y_1 \\
 y_{c2} &= a_5y_3 + a_6(a_4y_1 + a_3y_2) \\
 \theta_1 &= (y_1 - y_2)/s_1 \\
 \theta_2 &= (a_4y_1 + a_3y_2 - y_3)/s_2
 \end{aligned}
 \tag{6}$$

Substituting these geometric equations into equilibrium equations, the following six equations of motion are obtained for a tractor-trailer:

$$\begin{aligned}
 m_3\ddot{y}_4 + TF_1 - SF_1 &= 0 \\
 m_4\ddot{y}_5 + TF_2 - SF_2 &= 0 \\
 m_5\ddot{y}_6 + TF_3 - SF_3 &= 0
 \end{aligned}
 \tag{7}$$

$$\begin{bmatrix} c_1 & c_2 & c_3 \\ c_2 & c_4 & c_5 \\ c_3 & c_5 & c_6 \end{bmatrix} \begin{Bmatrix} \ddot{y}_1 \\ \ddot{y}_2 \\ \ddot{y}_3 \end{Bmatrix} = - \begin{Bmatrix} SF_1 \\ SF_2 \\ SF_3 \end{Bmatrix}$$

where

$$\begin{aligned}
 c_1 &= I_2a_4^2/s_2^2 + I_1/s_1^2 + a_2^2m_1 + a_3^2a_6^2m_2, \\
 c_2 &= I_2a_3a_4/s_2^2 - I_1/s_1^2 + a_1a_2m_1 + a_3a_4a_6^2m_2, \\
 c_3 &= a_4a_5a_6m_2 - I_2a_4/s_2^2,
 \end{aligned}$$

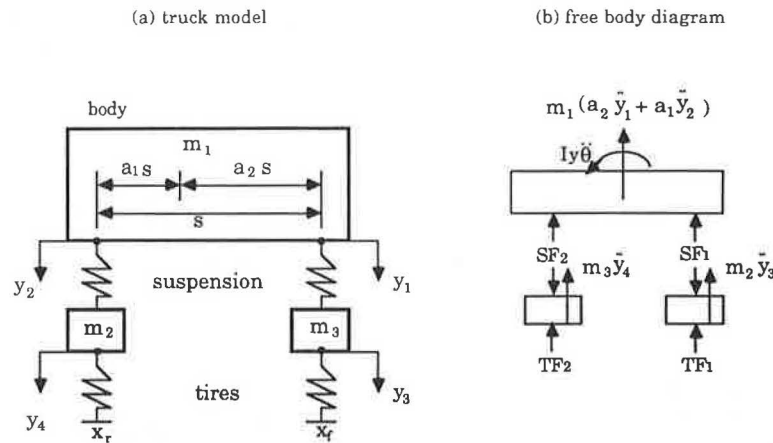
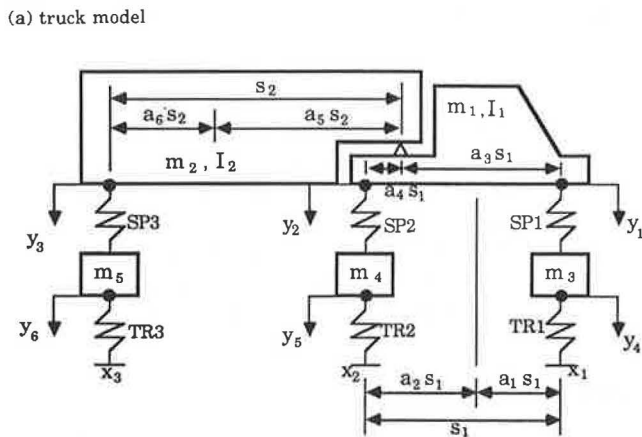


FIGURE 4 Model of a single truck.



(b) free body diagram

FIGURE 5 Model of a semi tractor-trailer.

$$c_4 = I_2 a_3^2 / s_2^2 + I_1 / s_1^2 + a_1^2 m_1 + a_3^2 a_2^2 m_2,$$

$$c_5 = a_3 a_5 a_6 m_2 - I_2 a_3 / s_2^2, \text{ and}$$

$$c_6 = a_5^2 m_2 + I_2 / s_2^2.$$

Table 1 gives the probability of occurrence for each truck type (12). It clearly indicates that the dominant type is a five-axle semi tractor-trailer. For each truck type, the calculations were based on truck weight measurement data (12), with the statistical parameters of the total weight given in Table 2. The weight distribution over axles and axle distances are assumed

TABLE 1 FREQUENCY OF OCCURRENCE FOR VARIOUS TRUCK TYPES

Truck Types	Frequency of Occurrence (%)
2-axle single (S2)	9
3-axle single (S3)	5
4-axle semi (T4)	19
5-axle semi* (T5)	67

* 5-axle semi tractor-trailer includes 6 or more axle semi tractor-trailers and 5-axle splits.

TABLE 2 STATISTICS OF TOTAL WEIGHT

Truck Type	Total Weight, W (kips)				
	Mean Value	Standard Deviation	Distribution Type	Minimum Value	Maximum Value
S2	15.26	4.42	Normal	10.0	30.0
S3	26.35	8.32	Normal	11.5	70.0
T4	27.99	8.06	Normal	13.7	70.0
T5	44.41	17.11	Normal	15.2	90.0

to be constant as shown in Table 3. The axles' own weights are assumed as constants with values taken from Francher and Ervin (11): 1,200 lb per front axle, 2,500 lb per mid axle, and 1,500 lb per rear axle.

ROAD ROUGHNESS

The road profile must be generated to analyze the effect of road surface roughness. The road profile is the realization of a random process and the surface roughness can be described by a spectral density function. The statistical model can be established using recent developments in profile measuring and spectral analysis.

TABLE 3 WEIGHT DISTRIBUTION AND AXLE DISTANCES

Truck Type	Weight Distribution (%)			Axle Distances (ft)
	Front	Middle	Rear	
S2	40	-	60	16.0
S3	31	-	69	18.2
T4	24	39	37	12.0, 29.7
T5	18	47	35	14.0, 33.1

In this study, the road surface is modeled as a stationary Gaussian random process (13). A stationary Gaussian random process, $X(t)$, can be generated using a simple periodic cosine function of time with amplitude α , circular frequency ω , and phase angle θ ,

$$X(t) = \alpha \cos(\omega t - \theta) \quad (8)$$

A finite sum of N discrete functions can also be considered

$$X(t) = \sum_{n=1}^N \alpha_n \cos(\omega_n t - \theta_n) \quad (9)$$

Assume the phase angle θ_n is an independent random variable distributed uniformly in the range of 0 to 2π . Then

$$E[\cos \theta_n] = \int_0^{2\pi} (\cos \theta_n) [1/(2\pi)] d\theta_n = 0 \quad (10)$$

Thus, the ensemble first two moments are

$$E[X(t)] = \sum_{n=1}^N \alpha_n E[\cos(\omega_n t - \theta_n)] = 0 \quad (11)$$

$$\begin{aligned} E[X^2(t)] &= E\left[\sum_{n=1}^N \alpha_n \cos(\omega_n t - \theta_n) \sum_{m=1}^M \alpha_m \cos(\omega_m t - \theta_m)\right] \\ &= \sum_{n=1}^N \frac{1}{2} \alpha_n^2 \end{aligned} \quad (12)$$

Both $E[X(t)]$ and $E[X^2(t)]$ do not depend on t ; hence the process $X(t)$ is stationary.

For a stationary Gaussian random process the following equation must be satisfied for the mean, m , variance, σ^2 , and spectral density function, $S(\omega)$:

$$\sigma^2 = \int_{-\infty}^{\infty} S(\omega) d\omega - m^2 \quad (13)$$

By substituting $m = 0$ and by discretizing the integral, the following equation is obtained:

$$\sigma^2 = 2 \sum_{n=1}^N S(\omega_n) \Delta\omega = E[X^2(t)] \quad (14)$$

Combining Equation 12 and Equation 14 yields

$$\alpha_n = \sqrt{4S(\omega_n) \Delta\omega} \quad (15)$$

Therefore, the random process $X(t)$ can be expressed as follows:

$$X(t) = \sum_{n=1}^N \sqrt{4S(\omega_n) \Delta\omega} \cos(\omega_n t - \theta_n) \quad (16)$$

Honda et al. (14) showed that the spectral density of the bridge surface roughness can be approximated by an exponential function. The spectral density $S(\gamma)$ can be represented by

$$S(\gamma) = a \cdot \gamma^{-n} \quad \gamma_a \leq \gamma \leq \gamma_b \quad (17)$$

where a is the roughness coefficient, n is the spectral shape index, γ is the spacial frequency, and γ_a and γ_b are the lower and upper limit. The statistics of a and n are shown in Table 4. From Equation 16 and Equation 17, the road profile can be generated by randomly selecting the phase angle θ . The roughness model does not include bumps or discontinuities.

BRIDGE DYNAMICS

It is assumed that the static and dynamic load distribution factors are the same. Consequently, the whole bridge is considered as a prismatic beam with flexural stiffness, EI . The equation of motion is

$$EI \frac{\partial^4 y}{\partial x^4} + \frac{\partial^2 y}{\partial t^2} = p(x, t) \quad (18)$$

where $p(x, t)$ = applied distributed force. This fourth order partial differential equation can be solved by the method of separation of variables. The general solution is

$$y(x, t) = \sum_{n=1}^{\infty} \phi_n(x) z_n(t) \quad (19)$$

In case of the simply supported beam, the shape function $\phi_n(x)$ is

$$\phi_n(x) = \sin(n\pi x/L) \quad (20)$$

TABLE 4 STATISTICS OF PARAMETERS IN SPECTRAL DENSITY FUNCTION

Parameter	Mean Value	Standard Deviation	Distribution Type	Minimum Value	Maximum Value
a	0.0098 $cm^2/c/m$		exponential	0.0	0.06
n	1.92	0.283	normal	1.3	2.5

Substituting Equation 19 and 20 into Equation 18 and including the damping effect, z_n , yields the following equation relating modal mass, $M_n = \int_{\phi} \phi_n^2(x)m dx = mL/2$, modal force, $F_n(t) = \int_{\phi} \phi_n(x)p(x, t) dx$, and natural frequency, $\omega_n = n^2\pi^2 \sqrt{EI/mL^4}$, flexural stiffness of the cross section, EI , and distributed applied force, $p(x, t)$:

$$\ddot{z}_n(t) + 2\xi_n\omega_n\dot{z}_n(t) + \omega_n^2z_n(t) = F_n(t)/M_n \quad (21)$$

The flexural stiffness is the most important parameter. However, it is difficult to evaluate EI because it depends on flexural stiffnesses of girders as well as transverse flexibility of the slab and diaphragms. EI can be calculated from the first flexural natural frequency of the bridge, f . The frequency, f (Hz), can be calculated for a given span length, L (m), using the formula established by Cantieni (15):

$$f = 95.4 \cdot L^{-0.933} \quad (22)$$

The stiffness can be calculated from the first natural frequency.

DYNAMIC LOAD FACTOR

A computer procedure was developed by the authors at The University of Michigan to calculate the maximum deflection (static and dynamic) and the DLF, following the flowchart shown in Figure 6. The program incorporates the equations describing dynamics of the vehicle, road roughness, and dynamics of the bridge. The Monte Carlo technique is used to generate basic parameters, including the road profile and the truck weight. The approach is demonstrated on a typical simply supported steel girder bridge with a 100-ft span. The first flexural frequency is 3.935 Hz (calculated using Equation 22). The n th order frequency is $n^2 \times 3.935$ Hz. The flexural stiffness can be calculated using continuous beam theory, $EI = 4.867 \times 10^{12}$ lb-in.². The damping of the bridge is assumed as 2 percent of the critical damping for each mode. In computations the time step used is 0.001 sec and the relative tolerance for convergence of each time step is 0.001. A typical example of a bridge response is shown in Figure 7.

The spectral density function is calculated for each road profile. However, an infinite number of road profiles can have the same spectral density. To examine the effect of different

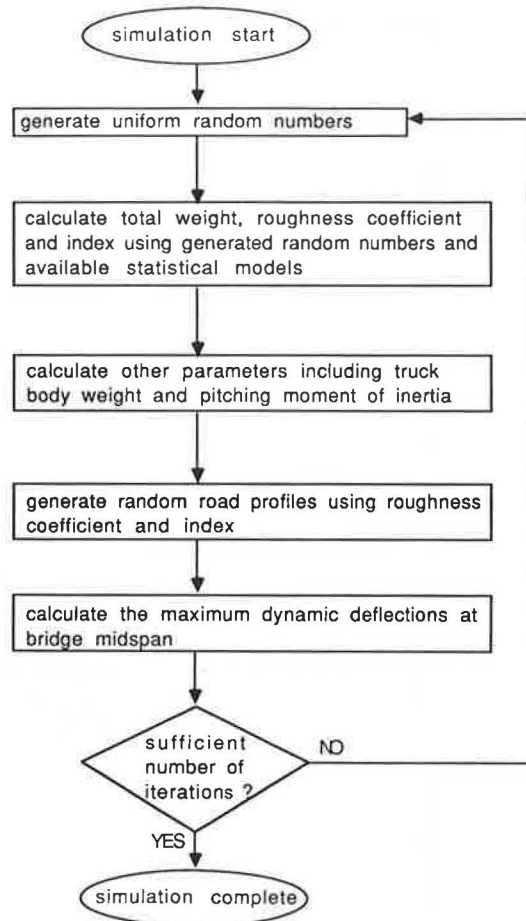


FIGURE 6 Flowchart of a computer simulation procedure.

profiles on the DLF, the calculations are carried out for randomly selected 10, 20, and 40 profiles. The resulting DLF values for a five-axle truck are plotted on the normal probability graph (13) in Figure 8. The vertical scale on the right is the cumulative probability (percentage). The vertical scale on the left is the inverse standard normal distribution. Normal and only normal distributions are represented by straight lines on this graph. The distributions plotted in Figure 8 indicate

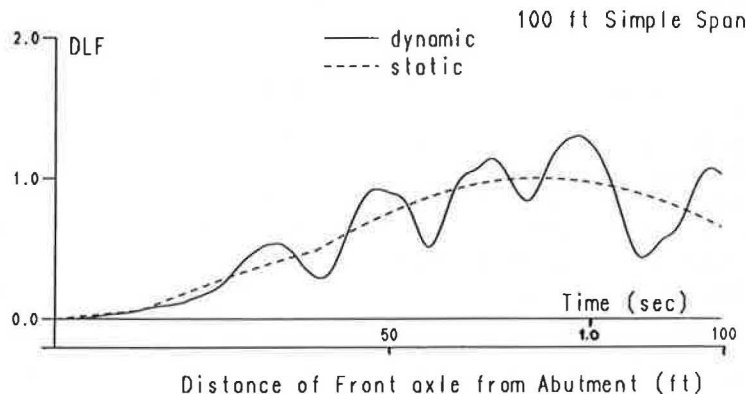


FIGURE 7 Typical example of bridge response for T5 truck.

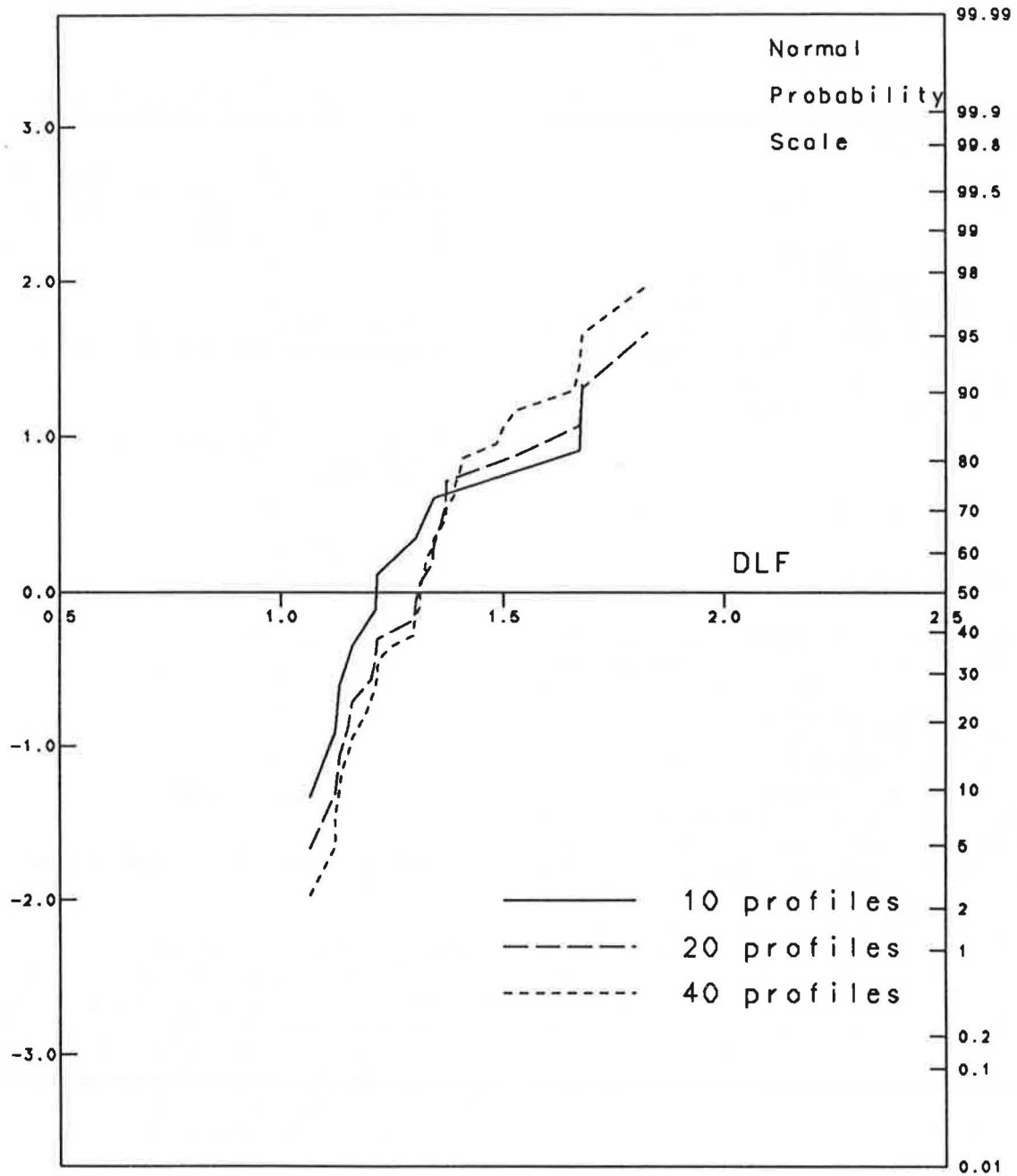


FIGURE 8 Dynamic load factor for various numbers of road profiles.

that 20 profiles provide a sufficient accuracy, and therefore it is used in further calculations.

Values of DLF are calculated separately for each truck type. For each type, 50 weights are generated, and for each weight, 20 road profiles are generated. This results in 1,000 DLF values per truck type. The DLF spectra for the considered truck types are plotted in Figure 9 on normal probability scale. The largest values of DLF were obtained for the single truck S2, and the lowest values for semi tractor-trailer T4. For each truck type, the mean and standard deviation of DLF are calculated and presented in Table 5. The large values are determined by bad surface conditions of existing bridges (14), and they are too high for design.

CONCLUSIONS

A procedure has been developed for calculation of the DLF. Three main factors are considered in the analysis: vehicle dynamics, road roughness, and bridge dynamics. The available test, measurement, and analytical data are reviewed and incorporated in computations. The developed method is demonstrated on a typical steel girder bridge. DLF values are generated using the Monte Carlo technique. It has been observed that simulation of 20 road profiles provided sufficiently accurate results. Spectra of DLF values have been calculated for the four most common truck types. The results are plotted on the normal probability graph.

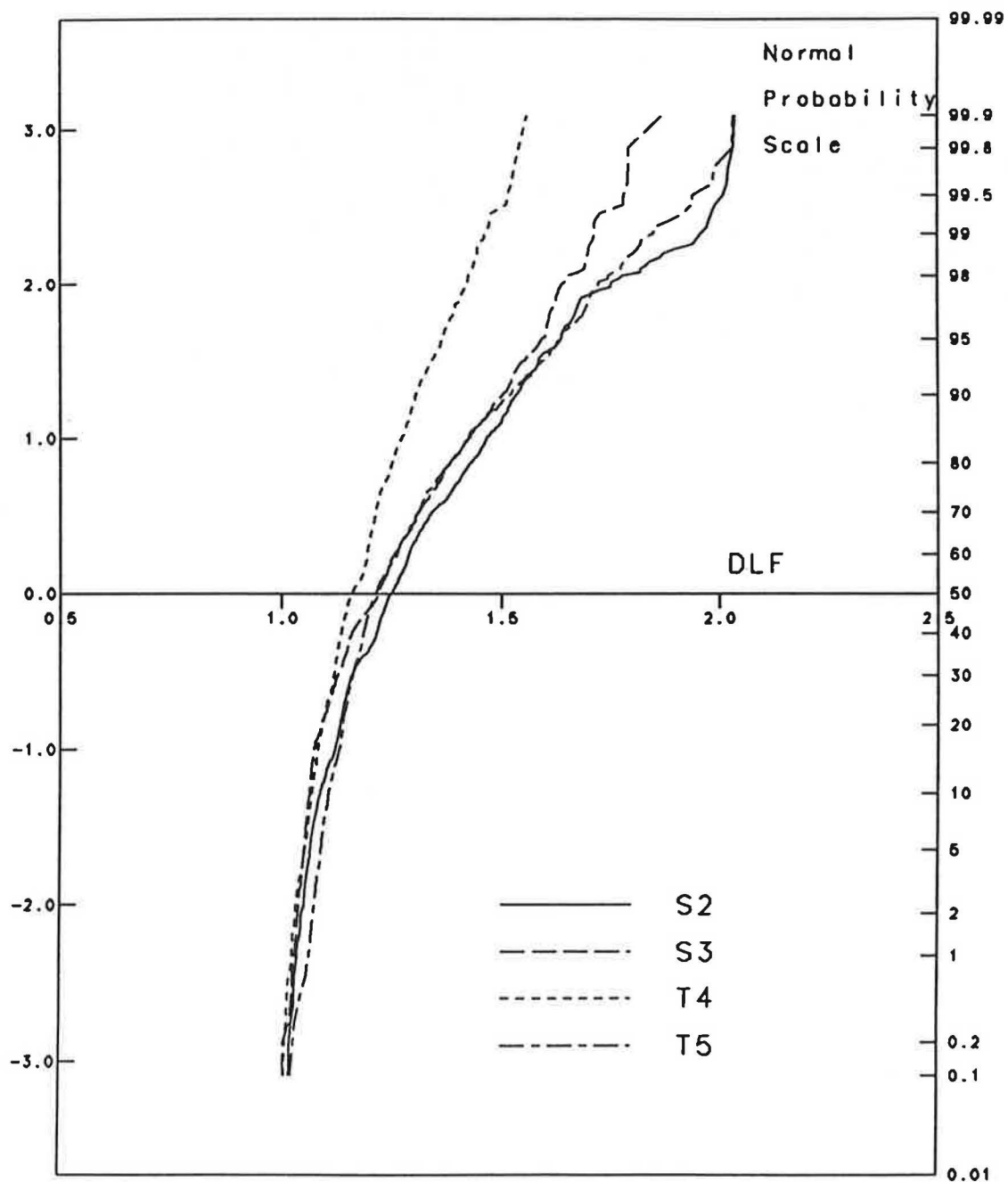


FIGURE 9 Dynamic load factor for various truck types.

TABLE 5 STATISTICS OF DYNAMIC LOAD FACTOR

Truck Type	Mean	Standard Deviation
S2	1.288	0.184
S3	1.249	0.168
T4	1.179	0.096
T5	1.271	0.171

The developed procedure provides an analytical tool for quantification of the dynamic load. The important application is in the development of efficient design and evaluation criteria. However, there is a need for more measurement data including vehicle characteristics and bridge response parameters.

ACKNOWLEDGMENTS

The presented research has been partially sponsored by the National Science Foundation with John B. Scalzi as program director, which is gratefully acknowledged.

REFERENCES

1. *Standard Specifications for Highway Bridges*. AASHTO, Washington, D.C., 1983.
2. *Ontario Highway Bridge Design Code*. Ministry of Transportation and Communications, Downsview, Ontario, Canada, 1983.
3. *Schweizer Norm*. Schweizer Ingenieur und Architekt, Nov. 1985.
4. J. R. Billing. *Dynamic Tests of Bridges in Ontario, 1980*. Research and Development Reports, Vol. 26. Ministry of Transportation and Communications, Downsview, Canada, 1982.
5. R. K. Gupta. Dynamic Loading of Highway Bridges. *Journal of the Engineering Mechanics Division*, ASCE, Vol. 106, No. EM2, April 1980, pp. 377-393.
6. D. J. Harman. *Survey of Commercial Vehicles Weights 1978 to 1982*. Report RR236. Ministry of Transportation and Communications, Downsview, Canada, Nov. 1985.
7. H. Honda, T. Kobori, and Y. Yamada. Dynamic Factor of Highway Steel Girder Bridges. *Proc., International Association of Bridge and Structural Engineering*, P-98/86, Zurich, Switzerland, May 1986, pp. 57-75.
8. T. Huang. Vibration of Bridges. *Shock and Vibration Digest*, Vol. 8, No. 3, 1976, pp. 61-76.
9. C. O'Connor and R. W. Pritchard. Impact Studies on Small Composite Girder Bridge. *Journal of the Structural Engineering Division* ASCE, Vol. 111, No. 3, March 1985, pp. 641-653.
10. P. S. Fancher, R. D. Ervin, C. C. MacAdam and C. B. Winkler. *Measurement and Representation of the Mechanical Properties of Truck Leaf Springs*. Technical Paper Series 800905. Society of Automotive Engineers, Warrendale, Pa., 1980.
11. P. S. Fancher and R. D. Ervin. *A Component Factbook for Straight and Articulated Heavy Trucks*. Report UMTRI-86-12. University of Michigan Transportation Institute, 1986.
12. F. Moses and M. Ghosn. *Instrumentation for Weighing Trucks-in-Motion for Highway Bridge Loads*. FHWA-OH-83-001, Final Report. FHWA, U.S. Department of Transportation, March 1983.
13. J. R. Benjamin and C. A. Cornell. *Probability, Statistics, and Decision for Civil Engineers*. McGraw-Hill Book Co., New York, 1970.
14. H. Honda, Y. Kajikawa and T. Kobori. Spectra of Road Surface Roughness on Bridges. *Journal of the Structural Engineering Division*, ASCE, Vol. 108, No. ST9, Sept. 1982, pp. 1956-1966.
15. R. Cantieni. *Dynamic Load Tests on Highway Bridges in Switzerland*. Report 211. Swiss Federal Laboratories of Materials Testing and Research, Dübendorf, 1983.

Publication of this paper sponsored by Committee on Dynamics and Field Testing of Bridges.